

1  
2  
3  
4  
5  
6  
7  
8  
9  
10  
11  
12  
13  
14  
15  
16  
17  
18  
19  
20  
21  
22  
23  
24  
25  
26  
27  
28  
29  
30  
31  
32  
33  
34  
35  
36  
37  
38  
39  
40  
41  
42  
43  
44  
45  
46  
47  
48  
49  
50  
51  
52  
53  
54  
55  
56  
57  
58  
59  
60

# Detecting Exosomes Specifically: A Multiplexed Device based on Alternating Current Electrohydrodynamic Induced *Nanoshearing*

*Ramanathan Vaidyanathan,<sup>‡</sup> Maedeh Naghibosadat,<sup>‡</sup> Sakandar Rauf, Darren Korbie, Laura  
G. Carrascosa, Muhammad J. A. Shiddiky, \*and Matt Trau\**

Australian Institute for Bioengineering and Nanotechnology (AIBN), Corner College and  
Cooper Roads (Bldg 75), The University of Queensland, Brisbane QLD 4072, Australia

Tel: +61-7-33464178; Fax: +61-7-33463973

\*Email: m.shiddiky@uq.edu.au (MJAS); m.trau@uq.edu.au (MT)

<sup>‡</sup> Authors contributed equally

**ABSTRACT**

Exosomes show promise as non-invasive biomarkers for cancers, but their effective capture and specific detection is a significant challenge. Herein, we report a multiplexed microfluidic device for highly specific capture and detection of multiple exosome targets using a *tunable* alternating current electrohydrodynamic (ac-EHD) methodology - referred to as *nanoshearing*. In our system, electrical body forces generated by ac-EHD act within nanometers of an electrode surface (*i.e.*, within the electrical layer) to generate nanoscaled fluid flow which enhances the specificity of capture and also reduce nonspecific adsorption of weakly bound molecules from the electrode surface. This approach demonstrates the analysis of exosomes derived from cells expressing human epidermal growth factor receptor 2 (HER2) and prostate specific antigen (PSA), and also capable of specifically isolating exosomes from breast cancer patient samples. The device also exhibited a 3-fold enhancement in detection sensitivity in comparison to hydrodynamic flow based assays (LOD 2750 exosomes/ $\mu$ L for ac-EHD *vs* LOD 8300 exosomes/ $\mu$ L for hydrodynamic flow; ( $n = 3$ )). We believe this approach can potentially find its relevance as a simple and rapid quantification tool to analyze exosome targets in biological applications.

**KEYWORDS**

AC electrohydrodynamics, exosomes, multiplex detection, microfluidic devices

## INTRODUCTION

Exosomes are membrane nanovesicles released from cells and are present in body fluids such as blood, urine and saliva.<sup>1</sup> They are believed to carry a cargo of proteins, lipids, mRNA, microRNA (miRNA) and transfer this cargo to recipient cells which alter the biochemical composition, signalling pathways, and genomic states of the recipient cells.<sup>2,3</sup> This could also enable them to engage in multiple cell-receptor (surface) interactions simultaneously. Exosomes can thus serve as extracellular messengers mediating cell-cell communication, raising the possibility of these enveloped exosomal receptors in body fluids as novel non-invasive biomarkers for cancer.<sup>3,4</sup> Although their physiological roles are still under investigation there is a growing need for reliable methods for accurate isolation and detection of exosomes from biological fluids. Current methods for the isolation and characterisation of exosomes (*e.g.*, ultracentrifugation, electron microscopy etc.) cannot discriminate between exosomes and other membrane vesicles, lipid structures, or retrovirus particles found in body fluids which are similar in terms of size and density.<sup>4,6</sup> More recently, several microfluidic approaches<sup>7-9</sup> using laminar flow based fluid micromixing have been reported to specifically isolate exosomes from biological fluids. Despite their excellent demonstrations, they are limited by their inability to manipulate surface shear forces to reduce nonspecific adsorption of cells or other molecules and provide quantitative information on these isolated nanovesicles. Therefore, a methodology that can effectively isolate and specifically detect these vesicles and their enveloped biomarkers in complex biological samples could provide further insights into the fundamental role and functions of these poorly understood, yet highly important biological vesicles.

Herein, we present a simple, multiplexed microfluidic platform to address these problems in current exosome detection methodologies. Our approach relies on the use of an alternating current (ac) electrohydrodynamic (ac-EHD) induced surface shear force which

engenders lateral fluid flow within few nanometers of an electrode surface.<sup>10-14</sup> Because this phenomenon involves a shear force within a few nanometers of the surface, we refer to it as *nanoshearing*. When samples containing target exosomes are driven through antibody-functionalized devices under ac-EHD flow (Figure 1), it provides the capability to specifically capture these exosomes by increasing the number of exosome-antibody (surface bound) collisions, which is a result of improved analyte transport. Since the magnitude of this force can be *tuned* externally via the application of frequency and/or amplitude, it can be applied to preferentially select specifically bound exosomes over nonspecifically adsorbed non-target species to surfaces (*i.e.*, non-target species bound weakly to the surface than that of the specifically captured exosomes). This method also provides the capability to simultaneously detect multiple exosome targets using a simple and rapid on-chip naked eye detection readout (*i.e.*, avoids use of any sophisticated instrumental readouts) based on the catalytic oxidation of peroxidase (*e.g.*, from horseradish peroxidase (HRP) conjugated detection antibody) substrate 3,3',5,5'-Tetramethylbenzidine (TMB).<sup>15</sup> Additionally, UV-Visible spectroscopy measurements from the colorimetric solutions provide quantitative analysis of multiple exosomes in a single assay format. The performance of our device for spiked exosome and patient serum samples was comparable with current exosome isolation and detection technologies.

## EXPERIMENTAL SECTION

**Reagents.** Unless stated otherwise, general-use reagents were purchased from Sigma Aldrich (Australia) and immunoassay reagents were obtained from R&D/Life Technologies (Burlington, ON), Thermo-Fisher Scientific (Australia), Abcam (Australia) and Invitrogen (Australia). All reagents and washing solutions used in the experiments were prepared using phosphate buffer saline (PBS, 10 mM, pH 7.4). Stock solutions of antibody were diluted in

1  
2  
3 PBS. Photoresists for fabrication (Microchem, CA) were used as per manufacturer's  
4  
5 instructions.  
6

7  
8 **Design of Multiplexed ac-EHD Devices.** In this study, we designed a multiplexed  
9  
10 microfluidic device containing asymmetric planar microelectrode pairs within a long  
11  
12 microchannel. The device contains three channels with individual inlet and outlet ports with  
13  
14 each channel comprising of 50 asymmetric planar electrode pairs (Figure S1, Supporting  
15  
16 Information). The small electrode of 50  $\mu\text{m}$  and large electrode of 250  $\mu\text{m}$  are separated by a  
17  
18 distance of 50  $\mu\text{m}$ . Adjacent electrode pairs in each segment are separated by a distance of  
19  
20 150  $\mu\text{m}$ . The narrow and wide electrodes of each asymmetric electrode pair in all three  
21  
22 channels are connected to individual gold connecting pads (Figure S1, Supporting  
23  
24 Information) that form the cathode and anode respectively. The critical gap ( $r_0$ ) between  
25  
26 small ( $d_1$ ) and large electrodes ( $d_2$ ) in each pair and the distance between adjacent electrode  
27  
28 pairs ( $r_1$ ) in the array influence the ac-EHD induced fluid flow and the associated  
29  
30 micromixing. Previously, Brown et al.<sup>16</sup> and Ramos et al.<sup>17</sup> have demonstrated that the fluid  
31  
32 flow rate is inversely proportional to the geometry of the electrodes. The asymmetry in  
33  
34 electrode geometry in our device was optimized to engender effective ac-EHD induced fluid  
35  
36 flow (*i.e.*, acts as a fluid pump) and micromixing within the channel, and was maintained  
37  
38 uniformly throughout each channel as:  $r_0/d_2 = 0.2$ ,  $r_1/d_2 = 0.6$ ,  $d_1/d_2 = 0.2$ , respectively. The  
39  
40 device design was made using Layout Editor (L-edit V15, Tanner research Inc., CA) and  
41  
42 written to a chrome mask (5" X 5"; Qingyi Precision Mask-making (Shenzhen) Ltd, China).  
43  
44  
45  
46  
47  
48  
49  
50

51  
52  
53 **Fabrication of Devices.** Devices were fabricated at the Queensland node of Australian  
54  
55 National Fabrication Facility (Q-ANFF node). Fabrication of the device involves a two-step  
56  
57 standard photolithographic process as outlined in Figure S2, Supporting Information.  
58  
59  
60

1  
2  
3  
4 **a. Fabrication of asymmetric gold electrode patterns.** Initially, a passivation layer of silicon  
5 dioxide (thickness- 300 nm) was deposited on silicon wafers (diameter- 100 mm; thickness-1  
6 mm; single-side polished) in an oxidation furnace. The wafers were then cleaned with  
7 sonication in acetone for 5 min, rinsed with isopropyl alcohol and water for another 2 min,  
8 and dried with the flow of nitrogen. A thin film of negative photoresist (AZnLOF 2070,  
9 Microchem, Newton, MA) was spin coated (3000 rpm for 30 s) onto the wafer and soft baked  
10 at 110 °C for 6 min. Subsequent UV exposure (280 mJ/cm<sup>2</sup>) using a mask aligner (EVG 620,  
11 EV Group GmbH, Austria) and development (AZ 726 developer for 3 min) revealed the  
12 exposed patterns without photoresist. Metallic layers of Ti (10 nm) and Au (200 nm) were  
13 deposited using an electron beam (e-beam) evaporator (Temescal FC-2000) under high  
14 vacuum conditions followed by lift-off using ethanol revealed the patterned gold electrodes.  
15 The wafers were then diced (ADT 7100 wafer precision dicer) to obtain individual devices.  
16 Devices were characterized by SEM analysis using a JEOL (model 6610) instrument  
17 operating at an accelerating voltage of 10 kV.  
18  
19  
20  
21  
22  
23  
24  
25  
26  
27  
28  
29  
30  
31  
32  
33  
34  
35

36 **b. Fabrication of Microfluidic Channels.** The fabrication of microfluidic channels (Figure  
37 S2, Supporting Information) involve a two-step process that include the (i) fabrication of an  
38 SU-8 master molds containing three independent microfluidic channels (width,  $w = 400 \mu\text{m}$ ;  
39 height,  $h = 300 \mu\text{m}$ ; length,  $l = 25 \text{ mm}$ ) with 1 mm diameter inlet and outlet ports, and (ii)  
40 fabrication of microfluidic channels on PDMS using the master molds. Initially, a layer of  
41 negative photoresist (SU-8 2150; MicroChem, MA) was spin coated (1800 rpm) onto a clean  
42 silicon wafer (diameter, 100 mm; thickness-1 mm; single-side polished). The wafer was soft  
43 baked through a series of step change in temperature (65 °C for 7 min, 95 °C for 60 min, 65  
44 °C for 5 min). Subsequent UV exposure (380 mJ/cm<sup>2</sup>) was followed by a post-bake step  
45 (from 65 °C for 5 min, 95 °C for 20 min, 65 °C for 3 min). To reveal the fluidic channels the  
46 wafers were developed in propylene glycol methyl ether acetate (PGMEA) for 45 min. These  
47  
48  
49  
50  
51  
52  
53  
54  
55  
56  
57  
58  
59  
60

1  
2  
3 SU-8 masters were then used as molds, on which polydimethylsiloxane (PDMS) prepolymer  
4 mixed with its crosslinker (ratio 10:1; Sylgard 184 kit, Dow Corning) was poured, degassed,  
5 and allowed to cure in a conventional oven at 65 °C for 2 h. The cured PDMS replicas were  
6 removed from the molds and 1 mm holes were punched into PDMS at either ends of the  
7 channel to define the inlet and outlet ports (diameter, 1 mm).  
8  
9  
10  
11  
12  
13  
14  
15  
16

17 **Cell Culture and Isolation of Exosomes.** Breast cancer (HER2(+): BT-474; HER2(-):  
18 MDA-MB-231) and prostate cancer (PSA(+): PC3) cell lines were maintained in  
19 microvesicles depleted serum free Media 171 (Gibco, UK) supplemented with Mammary  
20 Epithelial supplement (Gibco, UK), 1% Pencillin/streptomycin and grown in 5% CO<sub>2</sub> at 37  
21 °C. The conditioned medium from 10<sup>6</sup> cells was collected after 60 h and centrifuged at 2000  
22 × g for 30 min to eliminate cell contamination (*e.g.*, cells and debris). Exosomes were  
23 isolated using Total Exosome isolation reagent (Life Technologies) as per manufacturer's  
24 instructions. Briefly, the supernatant was transferred to a new tube and the isolation reagent  
25 was added to the tube in the ratio 2:1. The samples were incubated overnight at 4 °C followed  
26 by filtration using 0.22 μm filter and centrifugation at 10000 × g for 1 h to obtain exosome  
27 pellets. Exosome pellets were then resuspended in 100 μL PBS (10 mM, pH 7.0) and stored  
28 at -20 °C for further use.  
29  
30  
31  
32  
33  
34  
35  
36  
37  
38  
39  
40  
41  
42  
43  
44  
45  
46  
47

48 **Cryo-Transmission Electron Microscopy (Cryo-TEM).** For cryo-TEM, 4 μL of exosome  
49 preparations were directly adsorbed onto lacey carbon grids (Quantifoil, Germany) and  
50 plunged into liquid ethane, using an FEI Vitrobot Mark 3 (FEI Company, The Netherlands).  
51 Grids were blotted at 100% humidity at 4 °C for about 3-4 s. Frozen/vitrified samples were  
52 imaged using Tecnai T12 Transmission Electron Microscope (FEI Company) operating at an  
53 acceleration voltage of 120 kV. Images were taken at 30,000x magnification, (approximate  
54  
55  
56  
57  
58  
59  
60

1  
2  
3 dose of 13.6 electrons/Å<sup>2</sup>), using an FEI Eagle 4k CCD (FEI Company), and SerialEM image  
4  
5 acquisition software.  
6  
7

8  
9  
10 **Dynamic Light Scattering Analysis.** Exosome samples were prepared by spiking 1 μL of  
11  
12 isolated exosomes in PBS (10 mM, pH 7.0) to obtain the desired dilution (1:1000). The size  
13  
14 and zeta potentials of the nanovesicles were measured using a dynamic laser scattering (DLS)  
15  
16 instrument (Zetasizer 3000HSA, Malvern Instrument) at 25 °C under a refractive index of  
17  
18 1.33 and viscosity of 0.89 mPa.s .  
19  
20  
21

22  
23  
24 **Device functionalization.** Prior to functionalization, the electrodes were cleaned by  
25  
26 sonication in acetone for 5 min, rinsed with isopropyl alcohol and water for another 2 min,  
27  
28 and dried with the flow of nitrogen. The array of gold microelectrode pairs within the capture  
29  
30 domain of the channel were then modified with the capture antibody (*e.g.*, anti-HER2, anti-  
31  
32 CD9 and/or anti-PSA) using avidin-biotin chemistry (Figure 2) in a three step process.  
33  
34 Initially, devices were incubated in biotinylated BSA (200 μg/mL in PBS, Invitrogen)  
35  
36 solution for 2 h followed by coupling with streptavidin (100 μg/mL in PBS, Invitrogen) for 1  
37  
38 h at 37 °C. Streptavidin conjugated channels were then coated with biotinylated capture  
39  
40 antibody (*e.g.*, anti-HER2 and/or anti-PSA or anti-CD9; 10 μg/mL in PBS, R&D systems) for  
41  
42 another 2 h. Channel was flushed three times with PBS (10 mM, pH 7.0) to remove any  
43  
44 unbound molecules after each step. Each of the surface modification steps (*e.g.*, biotinylated  
45  
46 BSA, streptavidin, and capture antibody) was performed manually by filling the  
47  
48 microchannel with corresponding solution to specifically modify the array of gold electrodes  
49  
50 within the capture domain. PDMS containing the microchannels was then aligned manually  
51  
52 onto the electrodes and sandwiched between custom built device holders (Figure S3,  
53  
54  
55  
56  
57  
58  
59  
60



1  
2  
3 Supporting Information) for samples to be filled and withdrawn via inlet and outlet ports,  
4  
5 respectively.  
6  
7  
8  
9

10 **Exosome capture and detection.** The concentration of exosomes in the isolated pellets was  
11 obtained using qNano measurements performed as described previously.<sup>18</sup> Exosome samples  
12 were prepared by spiking 1  $\mu\text{L}$  of isolated exosomes in PBS (10 mM, pH 7.0) to obtain the  
13 desired dilution (1:1000). Concentration measurements were obtained by calibrating particle  
14 count rate recordings against a reference particle suspension (polystyrene beads,  $d = 115$  nm).  
15 Samples were then prepared by spiking designated volumes of isolated exosomes in PBS (1  
16 mM, pH 7.0) to obtain the desired sample dilutions (1:200 to 1:3000) in a given volume  
17 (500  $\mu\text{L}$ ). Serum samples (1 mL) of two breast cancer patients were obtained from Ventyx  
18 Wesley Research Institute Tissue Bank, Brisbane, Australia and stored in  $-80$   $^{\circ}\text{C}$  until further  
19 use. Immunohistochemical expression analysis suggested overexpression (3+: Patient A) and  
20 very low expression (1+; Patient B) of HER2 in these patient samples. The small and large  
21 electrodes within the long channel of the ac-EHD devices (Figure S1,S3, Supporting  
22 Information) were connected to a signal generator (Agilent 33220A Function Generator,  
23 Agilent Technologies, Inc., CA) *via* gold connecting pads. Samples were then placed in the  
24 inlet reservoirs of the devices and driven through the channel by applying ac-EHD field. The  
25 field strength was applied for 30 min with 15 min intervals (without fluid flow) for a total  
26 pumping time of approximately 2 h. Control experiments were performed in the absence of  
27 ac-EHD field under pressure driven flow conditions using a syringe pump (PHD 2000,  
28 Harvard apparatus). Detection antibody FITC conjugated anti-HER2 (2  $\mu\text{g}/\text{mL}$ ; Invitrogen,  
29 UK) was driven through the channels under ac-EHD and/or pressure driven flow conditions.  
30 For anti-PSA and/or anti-CD9 functionalized devices, the detection antibody HRP conjugated  
31 anti-PSA (2  $\mu\text{g}/\text{mL}$ ; abcam) and/or FITC conjugated anti-CD9 (2  $\mu\text{g}/\text{mL}$ ; abcam) was driven  
32  
33  
34  
35  
36  
37  
38  
39  
40  
41  
42  
43  
44  
45  
46  
47  
48  
49  
50  
51  
52  
53  
54  
55  
56  
57  
58  
59  
60

1  
2  
3 through the channels under ac-EHD fluid flow. anti-HER2 functionalized devices were  
4 imaged under a fluorescence microscope (Nikon eclipse Ni-U upright microscope) to obtain  
5 fluorescence images of the captured exosomes. anti-HER2 and/or anti-CD9 functionalized  
6 devices were then further incubated with anti-fluorescein HRP (1:1000; abcam) antibody for  
7 45 min. Channels were flushed three times with PBS (1 mM, pH 7.0) after subsequent steps  
8 to remove any unbound molecules. 80  $\mu$ L of 3,3',5,5'-tetramethylbenzidine (TMB) solution  
9 was driven through the channels manually and the colorimetric reaction was allowed to  
10 proceed for 5 min to facilitate naked eye detection from the resulting colour change in  
11 solution. The colorimetric solution was withdrawn manually from the device using a  
12 micropipette and collected in an eppendorf for subsequent absorbance measurements.  
13 Absorbance measurements were obtained using a UV-Visible spectrophotometer (Shimadzu  
14 UV-2450, Shimadzu Corp.) and absorbance data was acquired using UVProbe (Ver. 2.3.1)  
15 data acquisition software.  
16  
17  
18  
19  
20  
21  
22  
23  
24  
25  
26  
27  
28  
29  
30  
31  
32  
33  
34  
35

## 36 RESULTS AND DISCUSSION

37  
38 To investigate the applicability of *nanoshearing* phenomenon, we constructed a  
39 multiplexed microfluidic device (see Experimental for design and fabrication details; Figure  
40 3a,b and Figure S1,S2, Supporting Information) with three independent microchannels  
41 comprehending a long array of consecutively placed asymmetric electrode pairs within each  
42 channel. The device was sandwiched between custom built holders with the small and large  
43 electrodes within the long channel being connected to a signal generator (see Figure S3,  
44 Supporting Information for experimental setup). The application of an alternating potential  
45 difference to each pair of asymmetric electrodes results in a nonuniform electric field  $E$   
46 (Figure 1) that induces charges in the double layer ( $\lambda_D$  = Debye length). The lateral variation  
47 in the total amount of induced double layer charges and spatial distribution of charges on the  
48  
49  
50  
51  
52  
53  
54  
55  
56  
57  
58  
59  
60

1  
2  
3 electrode surface give rise to stronger lateral forces on the large electrode, resulting in fluid  
4  
5 flow towards the large electrode.<sup>10,16</sup> This lateral flow due to surface shear forces generated  
6  
7 within nanometers ( $\lambda_D = \sim 4$  nm, calculated for 1 mM phosphate buffer saline (PBS) using  
8  
9 Debye-Huckel approximation<sup>19</sup> and use of the equation described in ref.11) of an electrode  
10  
11 surface is unidirectional. This unidirectional flow causes analytes in solution to be dragged by  
12  
13 the flow, and their interaction with the surface is significantly enhanced (Figure 1).  
14  
15  
16

17  
18 To demonstrate the utility of *nanoshearing* effect for exosome detection, we tested the  
19  
20 capture and detection of exosomes obtained from breast cancer cell lines expressing human  
21  
22 epidermal growth factor receptor 2 (HER2), an important breast cancer therapeutic target.<sup>20</sup>  
23  
24 Exosomes were isolated (see Experimental for exosome isolation) from breast cancer cell line  
25  
26 BT-474 showing HER2 overexpression.<sup>21</sup> Western blotting analysis verified the HER2  
27  
28 expression in these BT-474 derived exosomes (data not shown). Characterization of the  
29  
30 isolated exosomes using cryo-Transmission Electron Microscopy (TEM) suggested that  
31  
32 predominantly these vesicles contained double-walled lipid membrane layers (Figure 3c).  
33  
34 Dynamic Light Scattering (DLS) measurements (Figure 3d) suggested that the large  
35  
36 population of exosomes (*e.g.*, 98±0.7%) falling within the size range of 30-350 nm with the  
37  
38 average vesicle size determined to be 111±3.07 nm. The morphological and physical  
39  
40 characteristics determined using these techniques corroborate with previous evidences<sup>22,23</sup>  
41  
42 suggesting that these nanovesicles are probably of exosomal origin and were used for further  
43  
44 capture experiments using multiplexed ac-EHD devices.  
45  
46  
47  
48  
49  
50

51  
52 The critical determinants that comprehend the tuning capability of surface shear  
53  
54 forces and concomitant micromixing include the ac frequency and amplitude. To determine  
55  
56 the optimal ac-EHD induced forces for exosome capture, the electrode surface on individual  
57  
58 channels of the device was initially functionalized (see Experimental and Figure 2 for  
59  
60 exosome capture and detection) with anti-HER2 capture antibody. Samples containing

1  
2  
3 isolated exosomes (1:200 in PBS; see Experimental for sample preparation) were driven  
4 through the devices under the frequency ( $f$ ) range of 600 Hz-100 kHz at constant amplitude  
5 ( $V_{pp}$ ) of 100 mV. The captured exosomes were detected via a rapid (~5 min) on-chip naked  
6 eye read-out obtained due to the oxidation of TMB. The colorimetric solution was collected  
7 manually from the device and the corresponding absorbance measurements using UV-visible  
8 spectroscopy measurements (maximum absorbance at 652 nm;  $A_{652nm}$ ) provided quantitative  
9 information on the captured exosomes. Figure 4a,b demonstrates spiked exosome samples  
10 under the frequency range of 600 Hz -100 kHz at  $V_{pp} = 100$  mV. Capture performance of the  
11 device was found to be a function of the applied frequency as observed from the initial sharp  
12 colour change to deep blue (600 Hz and 1 kHz in Figure 4a) and a gradual change in colour to  
13 a clear solution (1 kHz- 100 kHz in Figure 4a) with increase in frequency. UV-Visible  
14 spectroscopy measurements (Figure 4b, inset) and absorbance peak at 652 nm ( $A_{652nm}$ ; Figure  
15 4b) also demonstrated a similar trend in capture levels thereby further verifying these  
16 observations. The resulting higher level of capture at low field (e.g.,  $f = 1$  kHz and  $V_{pp} = 100$   
17 mV) is probably due to the effective stimulation of the fluid flow around the capture domain  
18 that can maximize the effective exosome-antibody collisions (a condition where shear force <  
19 antibody-exosome binding force). In contrast, at higher frequencies the ac-EHD forces (e.g.,  $f$   
20 = 100 kHz,  $V_{pp} = 100$  mV) result in stronger fluid flow which could ablate exosome  
21 recognition (a condition where shear forces > antibody-antigen affinity interaction) and  
22 decrease the capture level. Therefore, the ac-EHD force resulted from the frequency of 1 kHz  
23 and amplitude of 100 mV was used for further studies in demonstrating the application of ac-  
24 EHD induced *nanoshearing* phenomenon in detecting exosomes.

25  
26  
27 To validate the specificity and accuracy of exosome capture and detection, control  
28 experiments were performed under applied ac-EHD field strength of  $f = 1$  kHz and  $V_{pp} = 100$   
29 mV using samples spiked with (1:200 in PBS) and without exosomes. In the case of samples  
30  
31  
32  
33  
34  
35  
36  
37  
38  
39  
40  
41  
42  
43  
44  
45  
46  
47  
48  
49  
50  
51  
52  
53  
54  
55  
56  
57  
58  
59  
60

1  
2  
3 without exosomes, negligible nonspecific binding of the FITC conjugated detection antibody  
4 was observed under ac-EHD field as evident from the absorption spectra (red; Figure S4a,  
5 Supporting Information). Representative fluorescence images (see Experimental for details)  
6 of the detected exosomes and nonspecifically bound detection antibody are shown in Figure  
7 S4b,c, Supporting Information. To further investigate the specificity of detection, we  
8 performed additional control experiments using (i) devices functionalized without anti-HER2  
9 capture antibody and (ii) devices without FITC conjugated anti-HER2 detection antibody.  
10 Samples containing spiked exosomes (1:200 in PBS) were driven through the devices under  
11 the applied ac-EHD flow conditions ( $f = 1$  kHz and  $V_{pp} = 100$  mV). As can be seen in  
12 Figure S5a,b, Supporting Information, devices without capture (blue; Figure S5a, Supporting  
13 Information) and/or detection antibody (green; Figure S5b, Supporting Information) did not  
14 have a substantial effect in altering detection capabilities of the devices owing to negligible  
15 nonspecific binding of the detection antibody (*e.g.*, device without capture antibody) and the  
16 absence of HRP for TMB oxidation (*e.g.*, device without detection antibody) respectively.  
17 This data suggests that ac-EHD induced *nanoshearing* can facilitate specific capture of target  
18 exosomes by minimising background response from detection antibody.  
19  
20  
21  
22  
23  
24  
25  
26  
27  
28  
29  
30  
31  
32  
33  
34  
35  
36  
37  
38  
39  
40

41 Tetraspanin superfamily proteins (*e.g.*, CD9, CD63, CD81, CD82 etc.) are one of the  
42 most abundant protein markers found in exosomes isolated from virtually any cell type.<sup>1</sup> To  
43 investigate the selectivity of capture and detection, we performed capture experiments on  
44 anti-CD9 functionalized devices using exosomes isolated from HER2(+) BT-474 and  
45 HER2(-) MDA-MB-231 breast cancer cell lines. Figure S5c, Supporting Information,  
46 demonstrates capture performance of the device for spiked samples containing exosomes  
47 (1:200 in PBS) isolated from BT-474 and MDA-MB-231 cell lines. Under the applied field  
48 strength ( $f = 1$  kHz and  $V_{pp} = 100$  mV), the capture performance was found to be almost  
49 similar for exosome samples isolated from both BT-474 (black, Figure S5c, Supporting  
50  
51  
52  
53  
54  
55  
56  
57  
58  
59  
60

1  
2  
3 Information) and MDA-MB-231 (red; Figure S5c, Supporting Information) cell lines. These  
4  
5 results support the fact that our approach is highly selective considering the specific capture  
6  
7 of exosomes derived from HER2(+) and HER2(-) cell lines using anti-CD9 functionalized  
8  
9 devices. To further verify the selectivity and specificity of our approach, we then performed  
10  
11 an additional capture experiments on anti-HER2 functionalized devices using exosomes  
12  
13 isolated from HER2(-) MDA-MB-231 cell lines and observed a negligible capture levels  
14  
15 (blue; Figure S5c, Supporting Information). This is possibly due to the lack of HER2  
16  
17 expression in MDA-MB-231 cell lines and cell derived exosomes. This data indicates that our  
18  
19 approach is selective in capturing exosomes of interest in spiked samples, rather than any  
20  
21 associated microvesicles, cell debris or protein molecules that could have possibly been  
22  
23 isolated during the exosome extraction procedure.  
24  
25  
26  
27  
28

29  
30 To assess the dynamic range and lower limit of detection (LOD) of our device,  
31  
32 designated volumes of exosomes were spiked in PBS to obtain desired dilutions (1:200 to  
33  
34 1:3000) and run on anti-HER2-functionalized devices under the optimal ac field strength of  $f$   
35  
36 = 1 kHz and  $V_{pp} = 100$  mV. The approximate concentration of exosomes in these samples  
37  
38 was calculated from qNano measurements (see Experimental for details) and was found to  
39  
40 range from  $4.15 \times 10^4 - 2.76 \times 10^3$  exosomes/ $\mu$ L. Under the applied ac-EHD field,  
41  
42 colorimetric readouts (Figure 5a) and corresponding absorbance data (Figure 5b) indicate that  
43  
44 the device was sensitive enough to detect samples containing approximately  $>2760$   
45  
46 exosomes/ $\mu$ L (*i.e.*, 1:3000 in PBS). The linear dynamic range of detection was found to be  
47  
48  $2.76 \times 10^3$  (1:3000 in PBS) to  $4.15 \times 10^4$  exosomes/ $\mu$ L (*i.e.*, 1:200 in PBS) with the lower  
49  
50 limit of detection (LOD) approximately  $>2760$  exosomes/ $\mu$ L. The average number of  
51  
52 exosomes obtained from biological fluids (*e.g.*, plasma, cell culture media, serum, urine etc.)  
53  
54 range from  $8.0 \times 10^3$  to  $5.0 \times 10^5$  exosomes/ $\mu$ L.<sup>23,24</sup> Thus, this level of detection ( $>2760$   
55  
56 exosomes/ $\mu$ L) indicate that our method could potentially be suitable for analysing exosomes.  
57  
58  
59  
60

1  
2  
3 However, we believe further optimization to the protocol and device geometry (*e.g.*, length,  
4 width, and height of the channel; spacing between electrodes in the long array of asymmetric  
5 pairs) could further improve the capture performance of our device to meet clinically useful  
6 detection limits.  
7  
8  
9  
10  
11

12 We then compared the capture performance under the optimal ac-EHD flow to that of  
13 a hydrodynamic flow using a pressure-driven system (*via* a syringe pump) to drive fluid  
14 through the devices with the similar flow rate ( $7 \mu\text{Lmin}^{-1}$ ; an equivalent to the flow generated  
15 under the optimal ac-EHD field of  $f = 1 \text{ kHz}$  and  $V_{pp} = 100\text{mV}$ ). Samples containing two  
16 different concentrations of exosomes (1:200 and 1:1000 in PBS) were driven through the  
17 devices under ac-EHD and pressure driven flow conditions. Figure S6a,b, Supporting  
18 Information, shows the capture performance of the device under ac-EHD induced fluid flow  
19 and pressure driven flow conditions. For both concentrations, colorimetric detection and  
20 corresponding absorbance data yielded a 5-fold increase in capture level and a 3-fold  
21 enhancement in detection sensitivity (LOD = 2750 exosomes/ $\mu\text{L}$  for ac-EHD vs LOD = 8300  
22 exosomes/ $\mu\text{L}$  for hydrodynamic flow; ( $n = 3$ )) under ac-EHD in comparison with pressure  
23 driven flow based controls. The enhanced exosome capture with the use of ac-EHD induced  
24 fluid flow compared to the pressure driven flow based devices may be attributed to the  
25 synergistic effect of the geometric arrangements of the antibody-functionalized  
26 microelectrode pairs within the channel, ac-EHD induced *nanoshearing* and concomitant  
27 fluid mixing phenomena.  
28  
29  
30  
31  
32  
33  
34  
35  
36  
37  
38  
39  
40  
41  
42  
43  
44  
45  
46  
47  
48  
49

50 To demonstrate the multiplexing capability of our device and also further examine  
51 the effect of *nanoshearing* to capture low concentration of target exosomes in large excess of  
52 non-target exosomes, microvesicles and cellular proteins, individual channels of the device  
53 was functionalized (Figure 6a) with anti-HER2 (*e.g.*, channel-1) and anti-PSA (*e.g.*, channel-  
54 2) capture antibody. Target exosomes derived from a specific cell line (HER2(+)) and/or  
55  
56  
57  
58  
59  
60

1  
2  
3 PSA(+)) were spiked with large excess of non-target exosomes derived from two nonspecific  
4 cell lines. For channel 1, specific exosomes (1:3000 in PBS) derived from BT-474 were  
5  
6 spiked with two nonspecific exosomes (for both cases, 1:200 in PBS) from MDA-MB-231  
7  
8 and PC3 cell lines. For channel 2, exosomes (1:3000) derived from PC3 cell line were used as  
9  
10 target exosomes while exosomes (1:200) from MDA-MB-231 and BT-474 cell lines were  
11  
12 used as nonspecific targets. Figure 6a demonstrates duplex detection of spiked cell derived  
13  
14 exosome samples under the applied ac field strength of  $f = 1$  kHz and  $V_{pp} = 100$  mV. It was  
15  
16 clearly evident that the capture and detection performance of the device was highly  
17  
18 reproducible with the device being sensitive enough to detect low concentration (1:3000) of  
19  
20 target BT-474 (blue; channel-1, Figure 6a) and PC3 (green; channel-2, Figure 6a) derived  
21  
22 exosomes in the presence of non-target exosomes (15 fold higher concentration than target  
23  
24 exosomes). We also validated the specificity of capture by performing additional control  
25  
26 experiments on anti-HER2 functionalized devices using (i) samples spiked only with non-  
27  
28 target exosomes derived from MDA-MB-231 and PC3 cell lines (*i.e.*, without target BT-474  
29  
30 derived exosomes) in PBS (for both cases, 1:200) and (ii) only PBS buffer (*i.e.*, without  
31  
32 target and non-target exosomes). Under the applied field strength of  $f = 1$  kHz at  $V_{pp} = 100$   
33  
34 mV, a very low background response from the detection antibody (black; Figure S7,  
35  
36 Supporting Information) and/or nonspecific exosomes (red; Figure S7, Supporting  
37  
38 Information) was observed that further verified the high specificity of immunocapture. This  
39  
40 level of background response suggests that our method is applicable to detect exosomes at  
41  
42  $>1:3000$  concentration in the presence of 15-fold excess of nonspecific exosomes in the  
43  
44 heterogeneous samples. Thus, *nanoshearing* can be an effective tool for the enhancement of  
45  
46 target capture even at low concentrations and is comparable to the existing methodologies for  
47  
48 avoiding nonspecific adsorption using molecular coatings<sup>25</sup> and zwitterion complexes.<sup>26</sup>  
49  
50 Furthermore, this detection limit and device performance is comparable with recent  
51  
52  
53  
54  
55  
56  
57  
58  
59  
60



1  
2  
3 microfluidic technologies for capture and detection of extracellular vesicles from complex  
4 biological samples based on immunoaffinity capture,<sup>7</sup> silicon nanowires traps on  
5 micropillars,<sup>8</sup> and nanoporous membranes<sup>9</sup> that rely on size based exclusion and exosomal  
6 marker based immunocapture. Additionally, the key to the functionality and simplicity of our  
7 approach includes: (i) stimulation of fluid flow around the antibody-modified electrodes (*i.e.*  
8 fluid *nanoshearing* in the electrode/solution interface) improve the analysis performance of  
9 exosome targets *via* enhancing the number of sensor-target collisions as well as physically  
10 displacing nonspecifically adsorbed species from the electrode surface, (ii) use of a  
11 multiplexed device enables the analysis of multiple exosome targets isolated from complex  
12 biological fluids (*e.g.*, cell culture media, serum), and (iii) on-chip naked eye detection  
13 coupled with absorbance measurements provides a rapid quantification tool potentially suited  
14 for clinical analysis of these nanovesicles.

15  
16  
17  
18  
19  
20  
21  
22  
23  
24  
25  
26  
27  
28  
29  
30  
31  
32 Finally, to investigate the diagnostic potential of our method, we performed  
33 experiments using HER2(+) (Patient A) and HER2(-) (Patient B) breast cancer patient serum  
34 (see Experimental for sample details). Individual channels of the devices were functionalized  
35 with anti-HER2 capture antibody and samples (500  $\mu$ L for each channel) were driven through  
36 the devices (Patient A: channel-1; Patient B: channel-2) under optimal ac-EHD field strength  
37 ( $f = 1$  kHz and  $V_{pp} = 100$  mV). Colorimetric readouts (Figure 6b) suggested high capture  
38 levels in the HER2(+) Patient A sample whilst negligible capture levels were observed in  
39 HER2(-) Patient B serum. The corresponding absorbance measurements (Figure 6b)  
40 corroborate with these observations. The maximum absorbance ( $A_{652nm}$ ) data suggested that  
41 the approximate concentration of exosomes in these samples were  $2 \times 10^4$  (Patient A) and  $3.7$   
42  $\times 10^3$  exosomes/ $\mu$ L (Patient B), respectively. Furthermore, to verify the selectivity and  
43 specificity of capture, these patient serum samples (500  $\mu$ L) were driven through anti-CD9  
44 functionalized devices (Patient A: channel-1; Patient B: channel-2) under the optimal ac-

1  
2  
3 EHD field strength ( $f = 1$  kHz and  $V_{pp} = 100$  mV). In this case, the capture performance of the  
4 device was found to be almost similar (Figure 6c) for both patient (HER2(+)) and HER2(-)  
5 serum samples. The results obtained from anti-HER2 and anti-CD9 functionalized devices  
6 support the fact that our approach is selective and specific in isolating exosomes rather than  
7 any nonspecific microvesicles, cell debris or protein molecules present in the patient samples.  
8 These data indicate that our approach is potentially suitable for the isolation of exosomes  
9 from clinical samples and can find its relevance as a simple diagnostic tool in clinical  
10 settings.  
11  
12  
13  
14  
15  
16  
17  
18  
19  
20  
21  
22  
23

## 24 CONCLUSIONS

25  
26 We have developed a novel microfluidic platform technology for rapid, multiplexed  
27 and highly specific on-chip detection and quantification of exosomes using the unique  
28 capacity of ac-EHD induced *nanoshearing*. The versatility of our approach lies in (i) the use  
29 of asymmetric microelectrode pairs as fluid pumps (avoids use of additional pumps, valves,  
30 etc) and capture/detection domain during simultaneous capture of multiple target exosomes  
31 under ac-EHD induced fluid flow and (ii) the potential to be applicable for essentially any  
32 biochemical assay based on immunocapture (via modifying the device with any antibody  
33 specific to any disease biomarker). We demonstrate the ability of this approach to enhance  
34 the detection capabilities of the device (*e.g.*, approximately  $> 2750$  exosomes/ $\mu\text{L}$  and 5 fold  
35 increase in capture and detection performance in comparison to hydrodynamic fluid flow)  
36 and also specifically isolate exosomes from breast cancer patient samples. We envisage that  
37 this proof-of-concept study offering a *tunable* control of the target capture process and  
38 enabling the detection of multiple exosome targets can potentially establish its significance as  
39 a rapid exosome quantification tool that can find promising applications in cancer  
40 diagnostics.  
41  
42  
43  
44  
45  
46  
47  
48  
49  
50  
51  
52  
53  
54  
55  
56  
57  
58  
59  
60

**AUTHOR INFORMATION****Corresponding Authors**

\*Email: m.shiddiky@uq.edu.au (MJAS); m.trau@uq.edu.au (MT)

Tel: +61-7-33464178; Fax: +61-7-33463973

**Notes**

The authors declare no competing financial interest.

**ACKNOWLEDGEMENTS**

This work was supported by the ARC DECRA (DE120102503) and ARC DP (DP140104006). We acknowledge funding from the National Breast Cancer Foundation of Australia via National Collaborative Research Grants (CG-12-07). We also acknowledge Mr. Will Anderson and Ms. Rebecca Lane for performing the DLS and qNano measurements. The fabrication work was performed at Queensland node of the Australian National Fabrication Facility (Q-ANFF) and microscopy analysis was performed at the Australian Microscopy and Microanalysis Research Facility (AMMRF).

**ASSOCIATED CONTENT****SUPPORTING INFORMATION**

Design, fabrication, and additional data. This material is available free of charge via the Internet at <http://pubs.acs.org>.

1  
2  
3  
4  
5  
6  
7  
8  
9  
10  
11  
12  
13  
14  
15  
16  
17  
18  
19  
20  
21  
22  
23  
24  
25  
26  
27  
28  
29  
30  
31  
32  
33  
34  
35  
36  
37  
38  
39  
40  
41  
42  
43  
44  
45  
46  
47  
48  
49  
50  
51  
52  
53  
54  
55  
56  
57  
58  
59  
60  
**REFERENCES**

- (1) Théry, C.; Zitvogel, L.; Amigorena, S. *Nat. Rev. Immunol.* **2002**, *2*, 569.
- (2) Booth, A. M.; Fang, Y.; Fallon, J. K.; Yang, J. M.; Hildreth, J. E.; Gould, S. J. *J. Cell Biol.* **2006**, *172*, 923-35.
- (3) Skog, J.; Würdinger, T.; van Rijn, S.; Meijer, D. H.; Gainche, L.; Sena-Esteves, M.; Curry, Jr., W. T.; Carter, B. S.; Krichevsky, A. M.; Breakefield, X. O. *Nat. Cell. Biol.* **2008**, *12*, 1470-76.
- (4) Valadi, H.; Ekström, K.; Bossios, A.; Sjöstrand, M.; Lee, J. J.; Lötvall, J. O. *Nat. Cell Biol.* **2007**, *9*, 654-59.
- (5) Cantin, R.; Diou, J.; Bélanger, D.; Tremblay, A. M.; Gilbert, C. *J. Immunol. Methods*, **2008**, *338*, 21–30.
- (6) Théry, C.; Clayton, A.; Amigorena, S.; Raposo, G. *Current Protocols in Cell Biology*, ed. K. Morgan, John Wiley, New York, **2006**, p. UNIT 3.22.
- (7) Chen, C.; Skog, J.; Hsu, C.-H.; Lessard, R. T.; Balaj, L.; Würdinger, T.; Carter, B.S.; Breakefield, X. O.; Toner, M.; Irimia, D. *Lab Chip* **2010**, *10*, 505-511.
- (8) Davies, R. T.; Kim, J.; Jang, S. C.; Choi, E.-J.; Gho, Y. S.; Park, J. *Lab Chip* **2012**, *12*, 5202-5210.
- (9) Wang, Z.; Wu, H.-J.; Fine, D.; Schmülen, J.; Hu, Y.; Godin, B.; Zhang, J. X. J.; Liu, X.; *Lab Chip* **2013**, *13*, 2879-2882.
- (10) Vaidyanathan, R.; Shiddiky, M. J. A.; Rauf, S.; Dray, E.; Tay, Z.; Trau, M. *Anal. Chem.* **2014**, *86*, 2042-49.
- (11) Shiddiky, M. J. A.; Vaidyanathan, R.; Rauf, S.; Tay, Z.; Trau, M. *Sci. Rep.* **2014**, *4*, 3716.
- (12) Vaidyanathan, R.; Rauf, S.; Dray, E.; Shiddiky, M. J. A.; Trau, M. *Chem. Eur. J.* **2014**, *20*, 3721-29.

- 1  
2  
3 (13) Vaidyanathan, R.; Rauf, S.; Shiddiky, M. J. A.; Trau, M. *Biosens. Bioelectron.* **2014**, *61*,  
4  
5 184-91.  
6  
7  
8 (14) Rauf, S.; Shiddiky, M. J. A.; Trau, M. *Chem. Commun.* **2014**, *50*, 4813-15.  
9  
10 (15) Marquez, L. A.; Dunford, H. B. *Biochemistry*, **1997**, *36*, 9349-55.  
11  
12 (16) Brown, A. B. D.; Smith, C. G.; Rennie, A. R.; *Phys. Rev. E.* **2001**, *63*, 016305.  
13  
14 (17) Ramos, A.; González, A.; Castellanos, A.; Green, N. G.; Morgan, H., *Phys.Rev. E.* **2003**,  
15  
16 *67*, 056302.  
17  
18 (18) Seth Roberts, G.; Yu, S.; Zeng, Q.; Chan, L. C. L.; Anderson, W.; Colby, A. H.;  
19  
20 Grinstaff, M. W.; Reid, S.; Vogel, R. *Biosens. Bioelectron.* **2014**, *31*, 17-25.  
21  
22 (19) Hunter, R. J.; *Foundations of colloidal science*, Oxford University Press Inc., New York,  
23  
24 **1987**.  
25  
26 (20) Carlsson, H.; Nordgren, H.; Sjöström, J.; Wester, K.; Villman, K.; Begtsson, N. O.;  
27  
28 Ostenstad, B. Lundqvist, H.; Blomqvist, C., *Br J Cancer* **2004**, *90*, 2344-2348.  
29  
30 (21) Subik, K.; Lee, J. F.; Baxter, L.; Strzepek, T.; Costello, D.; Crowley, P.; Xing, L.; Hung,  
31  
32 M. C.; Bonfiglio, T.; Hicks, D. G.; Tang, P., *Breast Cancer* **2010**, *4*, 35-41.  
33  
34 (22) Coleman, B. M.; Hanssen, E.; Lawson, V. A.; Hill, A. F. *FASEB J.* **2012**, *26*, 4160-73.  
35  
36 (23) de Vrij, J.; Maas, S. L.; van Nispen, M.; Sena-Esteves, M.; Limpens, R. W.; Koster, A.  
37  
38 J.; Leenstra, S.; Lamfers, M. L.; Broekman, M. L. *Nanomedicine (Lond)*. **2013**, *8*, 1443-58.  
39  
40 (24) Huang, X.; Yuan, T.; Tschannen, M.; Sun, Z.; Jacob, H.; Du, M.; Liang, M.; Dittmar, R.  
41  
42 L.; Liu, Y.; Liang, M.; Kohli, M.; Thibodeau, S. N.; Boardman, L.; Wang, L. *BMC*  
43  
44 *Genomics.* **2013**, *14*, 319.  
45  
46 (25) Ostuni, E.; Chen, C. S.; Ingber, D. E.; Whitesides, G. M. *Langmuir* **2001**, *17*, 2828-  
47  
48 2834.  
49  
50 (26) Banerjee, I.; Pangule, R. C.; Kane, R. S. *Adv. Mat.* **2011**, *23*, 690-718.  
51  
52  
53  
54  
55  
56  
57  
58  
59  
60

**FIGURE CAPTIONS**

**Figure 1.** Schematic representation of ac-EHD induced tunable *nanoshearing* for the specific capture of exosomes (appeared as white spherical particles). The large and small electrodes in an asymmetric electrode pair form the cathode and anode (or *vice versa*) of an electrolytic cell. The application of an ac field  $E$  across the electrode pairs results in nonuniform forces on the large and small electrodes due to the lateral variation in number of induced charges and their spatial distribution with the resultant force giving rise to unidirectional movement towards the larger electrode. These shear forces generated within nanometers ( $\lambda_D$ ) of an electrode surface engender fluid flow vortices and induce fluid mixing that can displace weakly bound nonspecific species and hence termed as *nanoshearing*.

**Figure 2.** Schematic representation of device functionalization, exosome capture and colorimetric detection of captured exosomes.

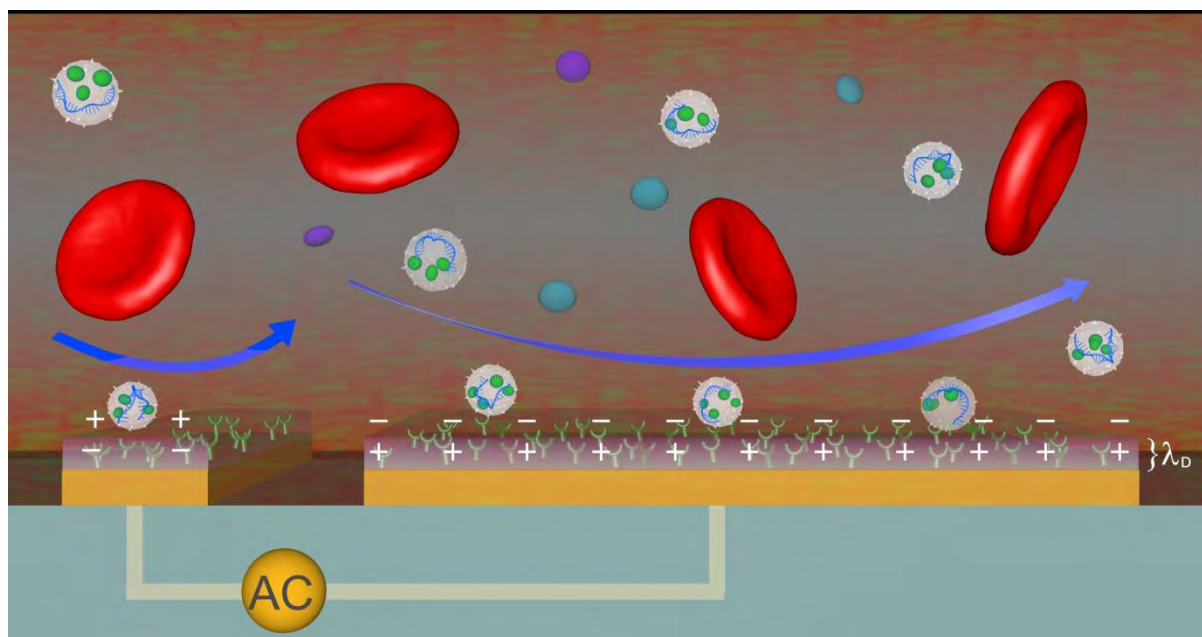
**Figure 3.** (a) Schematic of a multiplexed microfluidic device for exosome detection comprising of three independent channels. (b) Corresponding scanning electron microscopy (SEM) image of the enlarged segment of the device. (C) Cryo-TEM images of BT-474 cell derived exosomes demonstrating size and vesicular compartments such as membrane layers. (D) Dynamic light scattering measurements of BT-474 cell derived exosomes demonstrating the size range of the vesicles based on their scattered light intensity.

**Figure 4.** (a) Colorimetric detection of BT-474 cell derived exosomes spiked in 500  $\mu$ L PBS (1:200) under the frequency range  $f = 600$  Hz- 100 kHz at  $V_{pp} = 100$  mV. (b) Absorbance peak at 652 nm ( $A_{652nm}$ ) for exosomes spiked in PBS (1:200) under the frequency range  $f = 600$  Hz- 100 kHz at  $V_{pp} = 100$  mV. Each data point represents the average of three separate

1  
2  
3 trials ( $n = 3$ ) and error bars represent standard error of measurements within each experiment.  
4  
5  
6 Inset shows corresponding UV-Vis absorption spectra obtained from respective colorimetric  
7  
8 solutions.  
9

10  
11 **Figure 5.** (a) Colorimetric detection of samples containing spiked BT-474 cell derived  
12 exosomes in PBS at desired dilutions (1:200 to 1:3000) under ac-EHD field strength of  
13  $f = 1$  kHz at  $V_{pp} = 100$  mV. (b) Absorbance peak at 652 nm ( $A_{652nm}$ ) for the detected BT-474  
14 cell derived exosomes from spiked PBS samples at desired dilutions (1:200 to 1:3000) under  
15 ac-EHD field strength of  $f = 1$  kHz at  $V_{pp} = 100$  mV. Each data point represents the average  
16 of three separate trials ( $n = 3$ ) and error bars represent standard error of measurements within  
17 each experiment. Inset shows corresponding UV-Vis absorption spectra obtained from  
18 respective colorimetric solutions.  
19  
20  
21  
22  
23  
24  
25  
26  
27  
28  
29

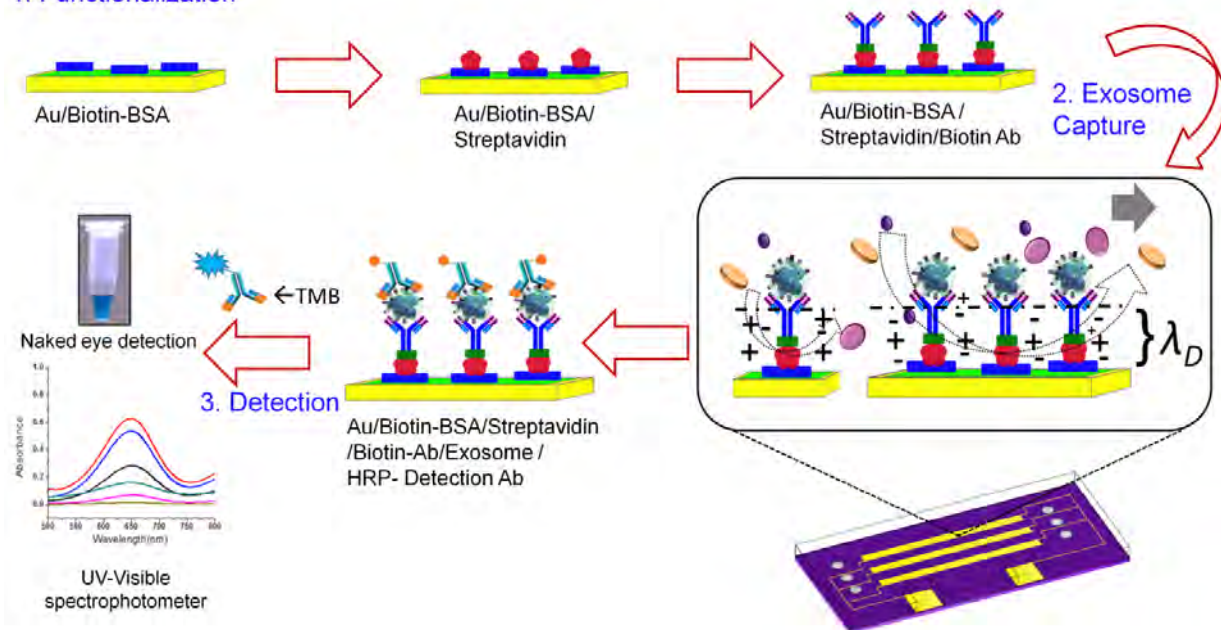
30  
31  
32 **Figure 6.** (a) UV-Vis absorption spectra of samples spiked with nonspecific exosomes  
33 derived from MDA-MB-231 (1:200) and PC3 or BT-474 (1:200) cell lines in PBS along with  
34 target HER2(+) BT-474 (blue; channel-1) or PSA(+) PC3 (green; channel-2) derived  
35 exosomes (1:3000) under the ac-EHD field strength of  $f = 1$  kHz at  $V_{pp} = 100$  mV. Inset  
36 shows naked eye detection of the captured BT-474 (channel-1) and PC3 (channel-2) derived  
37 exosomes under the applied ac-EHD field strength. (b,c) UV-Vis absorption spectra of  
38 HER2(+) (Patient A; red) and HER2(-) (Patient B; blue) breast cancer patient serum driven  
39 through (b) anti-HER2 and (c) anti-CD9 functionalized devices under the ac-EHD field  
40 strength of  $f = 1$  kHz at  $V_{pp} = 100$  mV. Inset shows naked eye detection of the captured  
41 exosomes.  
42  
43  
44  
45  
46  
47  
48  
49  
50  
51  
52  
53  
54  
55  
56  
57  
58  
59  
60



**Figure 1.**



## 1. Functionalization

**Figure 2.**

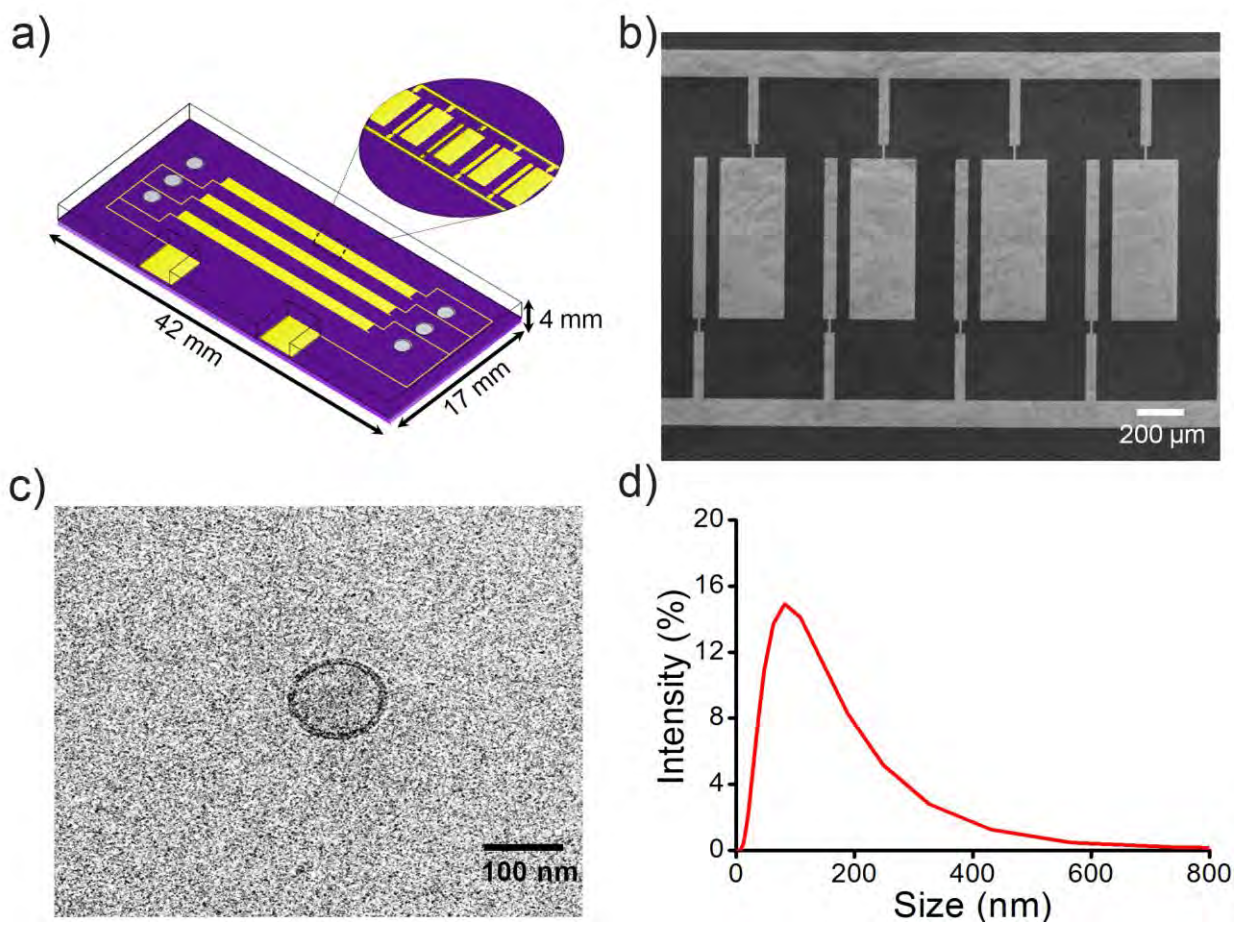
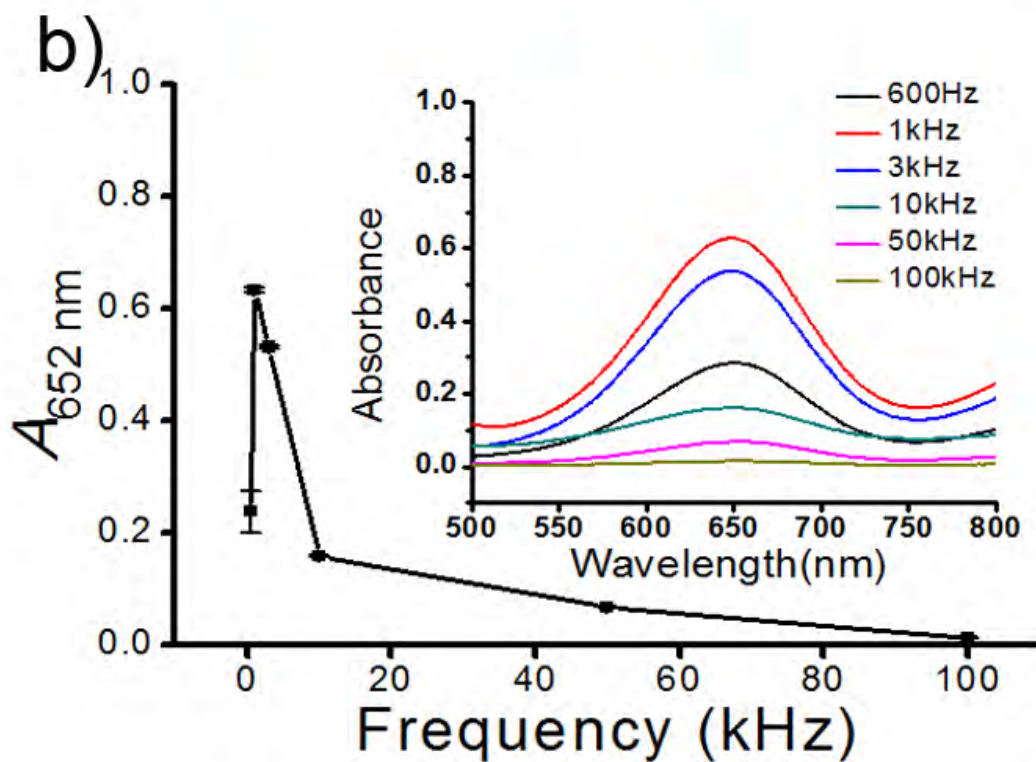
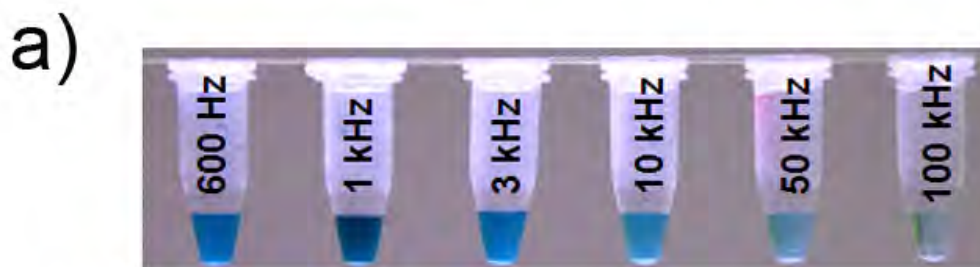


Figure 3.



46  
47  
48  
49  
50  
51  
52  
53  
54  
55  
56  
57  
58  
59  
60

Figure 4.

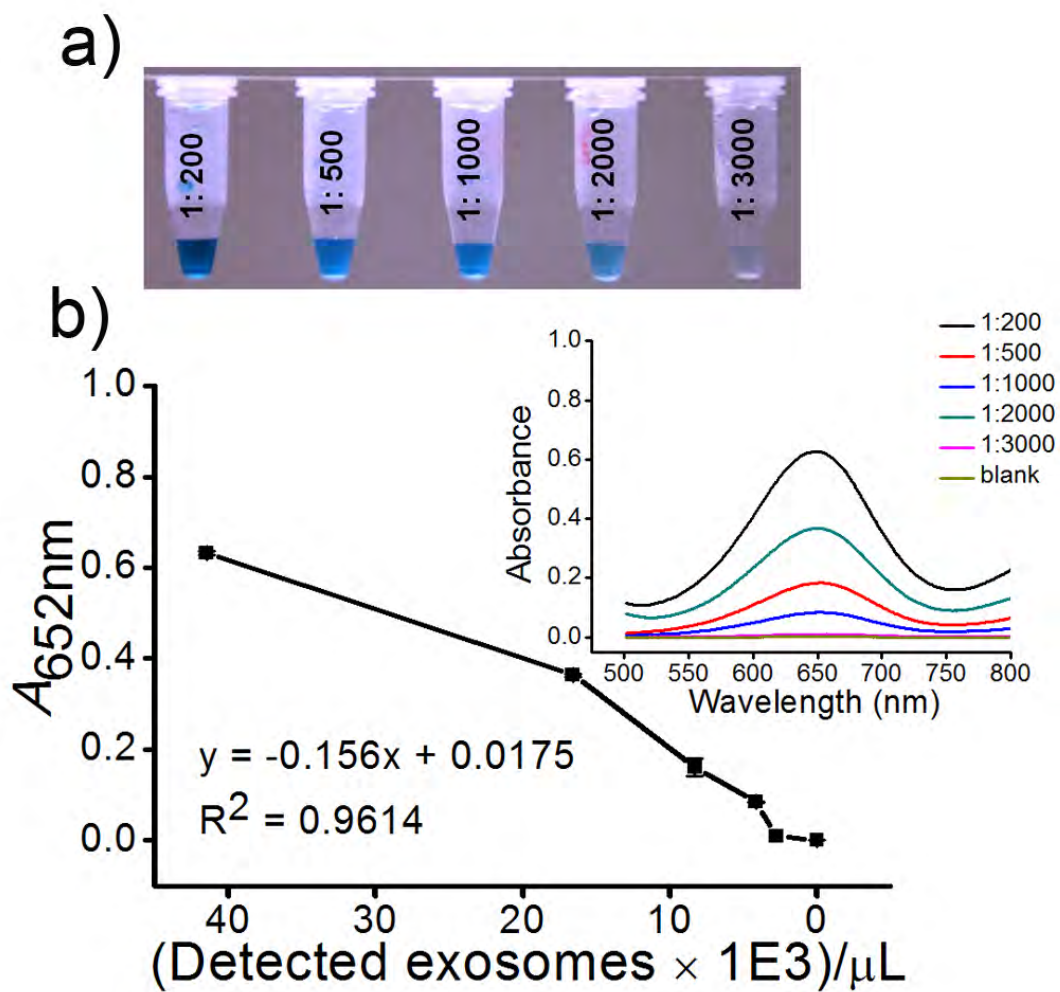


Figure 5.



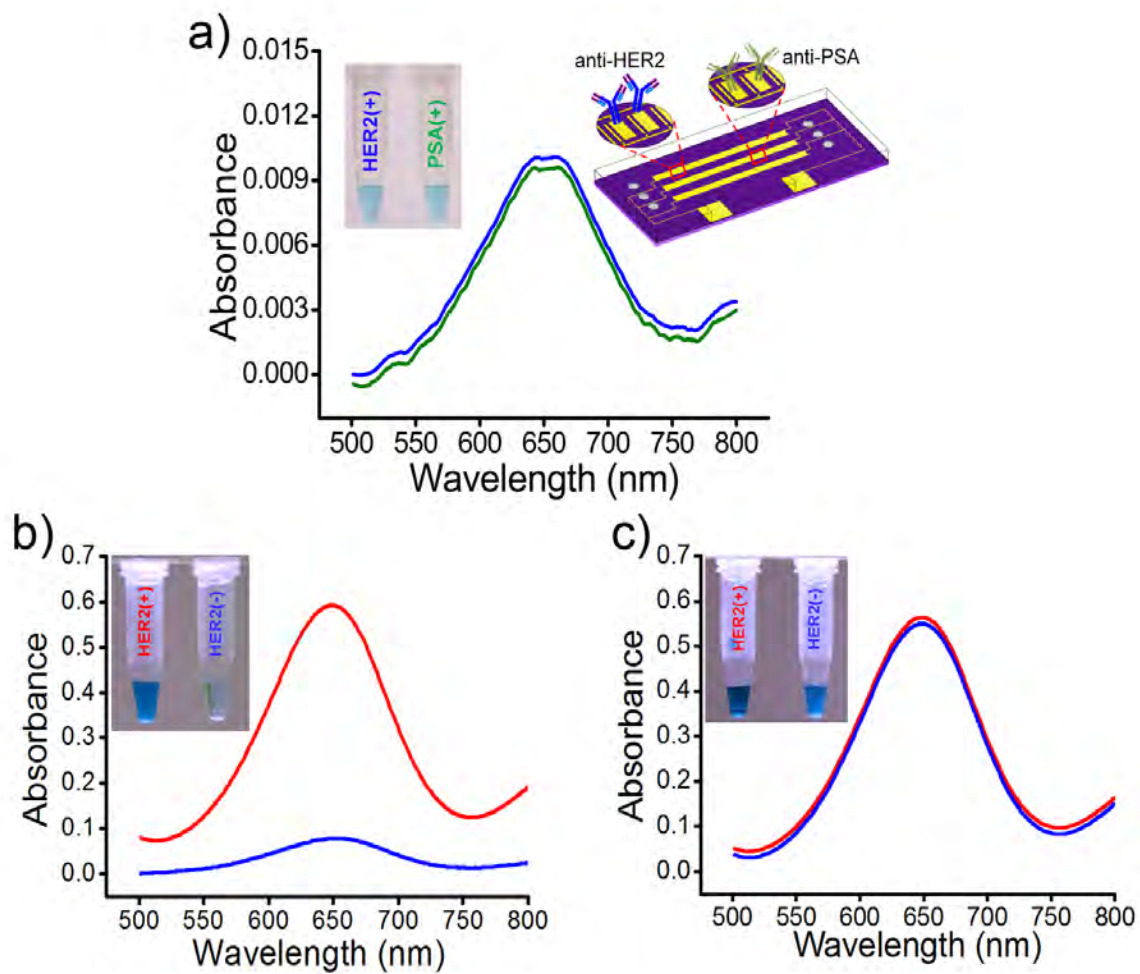


Figure 6.

1  
2  
3  
4  
5  
6  
7  
8  
9  
10  
11  
12  
13  
14  
15  
16  
17  
18  
19  
20  
21  
22  
23  
24  
25  
26  
27  
28  
29  
30  
31  
32  
33  
34  
35  
36  
37  
38  
39  
40  
41  
42  
43  
44  
45  
46  
47  
48  
49  
50  
51  
52  
53  
54  
55  
56  
57  
58  
59  
60

**For TOC only**

